

Angular momentum convergence of Korringa-Kohn-Rostoker Green's function methods

This article has been downloaded from IOPscience. Please scroll down to see the full text article.

2001 J. Phys.: Condens. Matter 13 3073

(<http://iopscience.iop.org/0953-8984/13/13/318>)

View [the table of contents for this issue](#), or go to the [journal homepage](#) for more

Download details:

IP Address: 171.66.16.226

The article was downloaded on 16/05/2010 at 11:45

Please note that [terms and conditions apply](#).

Angular momentum convergence of Korringa–Kohn–Rostoker Green’s function methods

Nassrin Y Moghadam¹, G M Stocks¹, X-G Zhang¹, D M C Nicholson¹,
W A Shelton¹, Yang Wang² and J S Faulkner³

¹ Oak Ridge National Laboratory, Oak Ridge, TN 37831-6114, USA

² Pittsburgh Supercomputing Center, 4400 5th Avenue, Pittsburgh, PA 15213, USA

³ Florida Atlantic University, Boca Raton, FL 33431, USA

Received 17 November 2000, in final form 19 February 2001

Abstract

The convergence of multiple-scattering-theory-based electronic structure methods (e.g. the Korringa–Kohn–Rostoker (KKR) band theory method), is determined by l_{max} , the maximum value of the angular momentum quantum number l . It has been generally assumed that $l_{max} = 3$ or 4 is sufficient to ensure a converged ground state and other properties. Using the locally self-consistent multiple-scattering method, which facilitates the use of very high values of l_{max} , it is shown that the convergence of KKR Green’s function methods is much slower than previously supposed, even when spherical approximations to the crystal potential are used. Calculations for Cu using $3 \leq l_{max} \leq 16$ indicate that the total energy is converged to within ~ 0.04 mRyd at $l_{max} = 12$. For both face-centred cubic and body-centred cubic structures, the largest error in the total energy occurs at $l_{max} = 4$; $l_{max} = 8$ gives total energies, bulk moduli, and lattice constants that are converged to accuracies of 0.1 mRyd, 0.1 Mbar, and 0.002 Bohr respectively.

1. Introduction

Multiple-scattering theory (MST) was first applied to electronic structure calculations by Korringa [1] in a theory now known as the Korringa–Kohn–Rostoker (KKR) band theory method [1, 2]. Recast in terms of Green’s function (GF) techniques, MST now underpins electronic structure methods for a wide variety of systems (e.g. ordered metals, substitutional alloys, surfaces, interfaces, and multi-layers) and physical properties (e.g. transport), as well as computer codes used for the interpretation of spectroscopies (e.g. LEED, EELS, photo-emission, and soft-x-ray) [3]. MST–GF techniques also underpin recently developed order- N methods for treating large systems [4–6] and a new full-potential version of the KKR band-structure method [7, 8] that yields results of an accuracy comparable to that of the all-electron FLAPW method.

In MST–GF calculations the primary convergence parameter is the cut-off l_{max} used in angular momentum expansions of the Green’s function, scattering t -matrix, and wave

functions. In the past, KKR calculations have typically been truncated at $l_{max} = 3$ or 4. There are several reasons for this. Firstly, the scattering phase shifts rapidly approach zero beyond the first few l -values ($l > 1$ for simple metals, $l > 2$ for transition metals, and $l > 3$ for f-electron elements) and thus do not contribute directly to the scattering. Secondly, utilizing higher l -values makes calculations so computationally demanding that they were not generally carried out. Finally, calculations with $l_{max} \leq 4$ have proved to be quite successful in explaining a wide variety of experimental results.

Despite the venerability and widespread use of MST–GF techniques, with a few notable exceptions, scant attention has been paid to their convergence properties with respect to l_{max} . The accuracy and convergence properties of MST, in the limit of $l_{max} \rightarrow \infty$, have been investigated by Butler [9] who performed calculations up to $l_{max} \sim 60$. He concluded that MST can be made arbitrarily accurate at some l_{max} . This study, however, is for the case of two muffin-tin scatterers, and more importantly, a two-centre expansion is used to ensure continuity at the boundaries between the wave functions inside and outside the cell. Unfortunately, these conclusions do not carry over to the present study, where the more conventional single-centre expansion is used. A more relevant study, that uses single-centre expansion, was carried out by Zeller *et al* [7], in which the full-potential tight-binding (TB) KKR method is used. They discuss the accuracy and convergence of the method and show numerical results for elemental copper and aluminium for values of $l_{max} = 4, 6$, and 8. We will discuss these results in more detail in the discussion section.

In this paper we present convergence test results that show that MST–GF methods converge more slowly than has been recognized even for spherical approximations to the cell potentials such as the muffin-tin (MT) approximation and the atomic sphere approximation (ASA). The calculations are facilitated by use of the locally self-consistent multiple-scattering (LSMS) method [4, 5]. The LSMS method is an order- N , real-space, MST–GF method originally developed for treating large systems. The particular feature of the LSMS method that allows accurate examination of l -convergence is the facility of using different l_{max} -values on different shells of atoms within the local regions surrounding each atom from which scattering is retained.

How the angular momentum cut-off enters MST–GF methods can most easily be seen by considering the site-diagonal single-particle Green's function. In the form advocated by Faulkner and Stocks [10] it is given by

$$G(\mathbf{r}, \mathbf{r}'; \epsilon) = \sum_{L, L'} Z_L^n(\mathbf{r}; \epsilon) \tau_{LL'}^{nm}(\epsilon) Z_{L'}^n(\mathbf{r}'; \epsilon) - \sum_L Z_L^n(\mathbf{r}; \epsilon) J_L^n(\mathbf{r}'; \epsilon). \quad (1)$$

The functions $Z_L^n(\mathbf{r}; \epsilon)$ and $J_L^n(\mathbf{r}; \epsilon)$ are solutions of the Schrödinger equation in the n th Wigner–Seitz cell, and the points \mathbf{r} and \mathbf{r}' are in that cell. In real space, the elements of the scattering path operator τ , $\tau_{LL'}^{nm}$ [11], are obtained by taking the inverse of the matrix \mathbf{M} :

$$\tau_{LL'}^{nm}(\epsilon) = [M(\epsilon)]^{-1}|_{LL'}^{nm} \quad (2)$$

whose general elements $M_{LL'}^{nm}(\epsilon)$ are given by

$$M_{LL'}^{nm}(\epsilon) = m_{LL'}^n(\epsilon) \delta_{nm} - g_{LL'}^{nm}(\epsilon). \quad (3)$$

The superscripts refer to the cells centred at the lattice sites \mathbf{R}_n and \mathbf{R}_m and the subscripts are a combination of the angular and azimuthal quantum numbers l, m . The matrix \mathbf{m}^n is the inverse of the scattering t -matrix for the atom on site n , and the elements of $\mathbf{g}(\epsilon)$ are the propagators for electrons in free space. For the special case of a one-atom-per-unit-cell periodic solid, the corresponding \mathbf{k} -space expressions take the form [12]

$$\tau_{LL'}^{nm}(\epsilon) = \frac{1}{\Omega_{BZ}} \int d\mathbf{k} \exp(i\mathbf{k} \cdot \mathbf{R}_{nm}) \tau(\mathbf{k}; \epsilon)|_{LL'} \quad (4)$$

and

$$\tau^{-1}(\mathbf{k}; \epsilon)|_{LL'} = M_{LL'}(\mathbf{k}; \epsilon) = m_{LL'}(\epsilon) - g_{LL'}(\mathbf{k}; \epsilon) \quad (5)$$

where the integration is over the Brillouin zone of volume Ω_{BZ} . In the above, $\mathbf{R}_{nm} = \mathbf{R}_m - \mathbf{R}_n$.

Clearly, l -truncation of the Green's function (1) enters in several places. Firstly, through truncation of the KKR matrix (3), the inverse of which yields the scattering path matrix (2). Secondly, through the truncation of the single-site wave functions $Z(\mathbf{r}'; \epsilon)$ and $J(\mathbf{r}'; \epsilon)$. The l -truncation, in turn, affects the cell densities of states $n(\epsilon)$ and the charge density $\rho(\mathbf{r})$ through

$$n(\epsilon) = -\frac{1}{\pi} \text{Im} \int_{\Omega_{WS}} G(\mathbf{r}, \mathbf{r}, \epsilon) d\mathbf{r} \quad (6)$$

and

$$\rho(\mathbf{r}) = -\frac{1}{\pi} \text{Im} \int_{-\infty}^{\epsilon_F} G(\mathbf{r}, \mathbf{r}, \epsilon) d\epsilon \quad (7)$$

where Ω_{WS} is the volume of the Wigner–Seitz cell, and ϵ_F is the Fermi energy. Finally the positioning of the Fermi energy is affected because it is determined from the condition

$$\mathcal{N}(\epsilon_F) = Z_{val} \quad (8)$$

where Z_{val} is the valence charge, and the integrated DOS, $\mathcal{N}(\epsilon)$, is given by

$$\mathcal{N}(\epsilon) = \int_{\epsilon_{\text{bottom}}}^{\epsilon} n(\epsilon') d\epsilon' \quad (9)$$

where ϵ_{bottom} denotes the bottom of the band. As will become clear later, it is in positioning the Fermi energy where l -truncation plays the largest role.

There is a way to reformulate the expression for the integrated density of states so that it will converge more rapidly in l . This requires the use of the Lloyd formula [13]

$$\mathcal{N}(\epsilon) = \mathcal{N}^0(\epsilon) + \frac{1}{N\pi} \text{Im} \ln \det \mathbf{M}(\epsilon) \quad (10)$$

where $\mathcal{N}^0(\epsilon)$ is the integrated DOS for free electrons and N is the number of atoms in the system. The Lloyd formula has the advantage that it yields the integrated DOS directly. It has the disadvantage that the charge obtained by integrating the Green's function over energies below the chemical potential, as determined by the Lloyd formula, will not have the correct integrated number of electrons. For finite systems or defects of finite extent, this discrepancy is of little consequence. For infinite systems, the charge discrepancy must be dealt with because it results in an infinite contribution to the Coulomb energy. Furthermore, the Lloyd formula cannot be applied locally to determine the integrated density on a site in a way that parallels the single-site density of states obtained from the Green's function. Thus, the angular momentum convergence of the Green's function is necessary for most MST calculations.

2. Computational techniques

Although the systems that are treated in this paper are metals for which the electronic structure is normally obtained using band theory, the l -convergence can also be studied rather efficiently using a technique that had its origin in the LSMS method [4, 5]. The feature of the LSMS method that greatly facilitates study of the angular momentum convergence is the manner in which the KKR matrix is constructed. When calculating the Green's function for a particular site n , only scattering from a finite number of surrounding atoms is retained. In this case

$$\tau(\epsilon)|_{\Gamma}^{nn} = [\mathbf{m}(\epsilon) - \mathbf{g}(\epsilon)]^{-1}|_{\Gamma}^{nn} \quad (11)$$

where τ , \mathbf{m} , and \mathbf{g} are matrices in both angular momentum and site index, and Γ denotes the number of atoms retained in the region around the atom in question which is referred to as the local interaction zone (LIZ). This procedure is used for each of the atoms in the system. For a system in which all of the atoms are the same, the electronic states need to be calculated at the centre of only one LIZ. Figure 1 shows a supercell with N atoms. The LIZ contains nine atoms ($\Gamma = 9$): one at the centre, four on the first-neighbour shell, and four on the second-neighbour shell; atoms outside the LIZ are shaded.

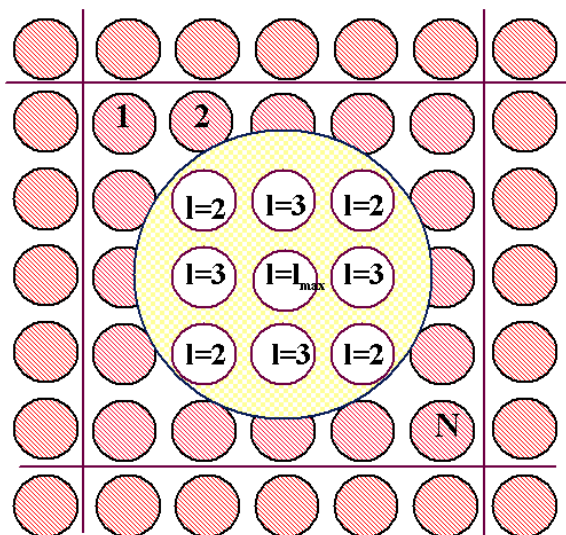


Figure 1. A supercell with N atoms. The atoms outside the local interaction zone (LIZ) are shaded. The LIZ contains nine atoms ($\Gamma = 9$). The KKR matrix is constructed by putting $l_{max} = 3$ on the centre and on the first-neighbour shell. $l_{max} = 2$ is put on the second-neighbour shell.

The dimensions of the block matrices that make up the KKR matrix are determined by the number of atoms on a given shell and the angular momentum cut-off on that shell. As the picture indicates, different l s can be put on different shells within the LIZ. To investigate convergence of the angular momentum in such system, it will be sufficient to vary the angular momentum cut-off only at the centre and first-neighbour shell. The l_{max} for the remaining shells within the LIZ need not change. This will allow electronic structure calculations at large l with modest additional computational cost. The convergence properties of the LSMS method with respect to the l_{max} retained on the outer shells of the LIZ is shown in table 1. Clearly $l_{max} = 3$ on the second-neighbour shell is sufficient to ensure <0.02 mRyd accuracy. For the case in question, previous studies [5] have shown that for the third shell and beyond, $l_{max} = 2$ is sufficient to ensure a similar convergence.

Table 1. Convergence of the LSMS method with respect to the l_{max} retained on the shells within the LIZ. Calculations are for the fcc Cu at $a = 6.76$ Bohr using the MT approximation. $\Gamma = 87$ atoms (central site plus six neighbour shells).

0	l_{max} on shell						Total energy + 3275 (Ryd)
	1	2	3	4	5	6	
4	3	3	2	2	2	2	-0.76993613
4	4	3	2	2	2	2	-0.77152820
4	4	4	2	2	2	2	-0.77154703
8	3	3	2	2	2	2	-0.76207045
8	8	3	2	2	2	2	-0.76428718
8	8	8	2	2	2	2	-0.76430975

3. Results

In the following, self-consistent-field (SCF) total-energy calculations are carried out for metallic copper in the face-centred cubic (fcc) and hypothetical body-centred cubic (bcc) structures. The choice $\Gamma = 87$ (89) is adequate to obtain better than 0.5 mRyd accuracy for the total energy for fcc (bcc) copper [5]; this corresponds to the central site plus six (seven) neighbour shells. Keeping in mind the previous discussion, only l_{max} for atoms at the centre and on the first-neighbour shell are varied. The l_{max} -values for the second and remaining shells are held fixed at 3 and 2 respectively.

To illustrate the convergence properties, we study the error in the total energy, ΔE_{tot} , Fermi energy, $\Delta \epsilon_F$, and integrated density of states, $\Delta \mathcal{N}$. Calculations having $l_{max} = 3$ on the central site and first-neighbour shell are used as references. Specifically, ΔE_{tot} , $\Delta \epsilon_F$, and $\Delta \mathcal{N}$ are defined as

$$\begin{aligned}\Delta E_{tot} &= E_{tot}^{l_{max}} - E_{tot}^{l_{max}=3} \\ \Delta \epsilon_F &= \epsilon_F^{l_{max}} - \epsilon_F^{l_{max}=3} \\ \Delta \mathcal{N} &= \mathcal{N}^{l_{max}}(\epsilon_F^{l_{max}=3}) - \mathcal{N}^{l_{max}=3}(\epsilon_F^{l_{max}=3}) = \mathcal{N}^{l_{max}}(\epsilon_F^{l_{max}=3}) - Z_{val}.\end{aligned}\quad (12)$$

In these equations $E_{tot}^{l_{max}}$ is the total energy calculated with $l = l_{max}$ on the central and first-neighbour sites, $E_{tot}^{l_{max}=3}$ is the total energy calculated with $l_{max} = 3$ on those sites, and $\epsilon_F^{l_{max}}$ and $\epsilon_F^{l_{max}=3}$ are their corresponding Fermi energies. $\mathcal{N}^{l_{max}}(\epsilon_F^{l_{max}=3})$ is the integrated density of states calculated at l_{max} while the Fermi energy is kept fixed at $\epsilon_F^{l_{max}=3}$.

Figure 2 shows the convergence behaviour of ΔE_{tot} , $\Delta \epsilon_F$, and $\Delta \mathcal{N}$ for fcc Cu having a lattice parameter $a = 6.76$ Bohr, $\Gamma = 87$, and using the MT approximation. From this figure it can be seen that ΔE_{tot} and $\Delta \epsilon_F$ decrease by several mRyd from $l_{max} = 3$ to 4 and increase on the same scale from $l_{max} = 4$ to 8. For $l_{max} > 8$ the convergence levels off and calculations

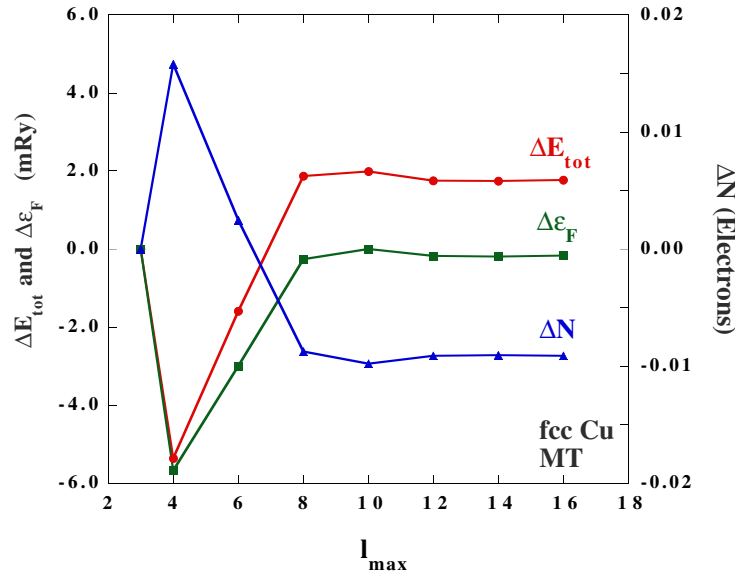


Figure 2. Convergence properties of ΔE_{tot} , $\Delta \epsilon_F$, and $\Delta \mathcal{N}$ as functions of the maximum angular momentum cut-off l_{max} . Calculations for $l_{max} = 3$ are used as a reference. The results are for fcc Cu, $a = 6.76$ Bohr, the MT approximation, and $\Gamma = 87$.

with $l_{max} = 8$ (12) are converged to within 0.1 (0.02) mRyd of $l_{max} = 16$. $\Delta\mathcal{N}$ exhibits opposite behaviour. It increases from $l_{max} = 3$ to 4, and decreases sharply for $4 \leq l_{max} \leq 8$. Beyond $l_{max} = 8$ the error is less than 0.0004 electrons. From the previous discussion it is clear that the error in the integrated DOS is the driver. This error results in a misplacement of the Fermi energy which, in turn, results in the error in the total energy.

Studies of bcc Cu ($a = 5.37$ Bohr and $\Gamma = 89$) exhibit very similar behaviour. Figure 3 shows ΔE_{tot} for both fcc and bcc structure. In addition, we show the structural energy difference $\Delta E_{fcc-bcc} = \Delta E_{fcc} - \Delta E_{bcc}$. While the changes in structural energy are smaller than the errors in the individual fcc and bcc total energies, reasonable convergence is not reached until $l_{max} \geq 10$, and the errors associated with $l_{max} = 3$ and 4 are of the order of 50%.

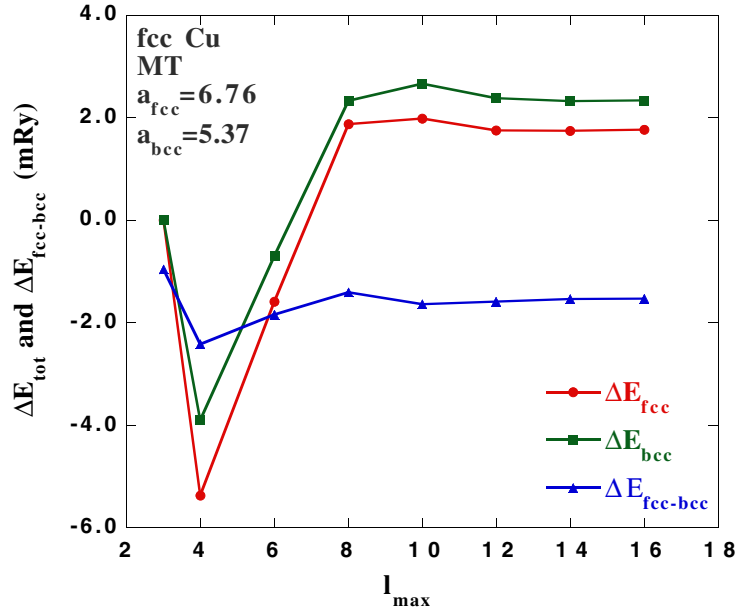


Figure 3. Convergence properties of ΔE_{tot} for fcc (circles) and bcc (squares), and the structural energy $E_{fcc} - E_{bcc}$ (triangles) for Cu. The fcc (bcc) lattice parameter is taken to be $a = 6.76$ (5.37) Bohr, $\Gamma = 87$ (89), and the MT approximation is used.

In all of the above, it should be stressed that the calculations are for a spherical approximation to the crystal potential, namely, the MT approximation. Similar results are obtained for the other often-used spherical approximation, namely the ASA. In figure 4 we show results for the ASA analogous to those of figure 2 for the MT approximation. The overall scale of the convergence behaviour of the ASA is the same as that for the MT approximation. However, it is generally of the opposite sign and is monotonic.

Of particular note is the convergence behaviour of \mathcal{N} . For the ASA, the error in the integrated density of states increases uniformly from $l_{max} = 3$ whilst for the MT approximation the error first increases at $l_{max} = 4$ and then decreases uniformly. The behaviour of the ASA is what one would expect on the basis of simple arguments and the behaviour of the underlying phase shifts. Recall that $\Delta\mathcal{N}$ is calculated with respect to the $l_{max} = 3$ results. For Cu, the phase shifts for $l_{max} > 3$ are small but positive. From the Friedel sum rule, one would expect these higher l -components to contribute a positive density of states, leading to an increase in the integrated density of states. A corollary of this is a monotonic decrease in the true Fermi energy, which is also observed. Clearly, the MT results do not follow the

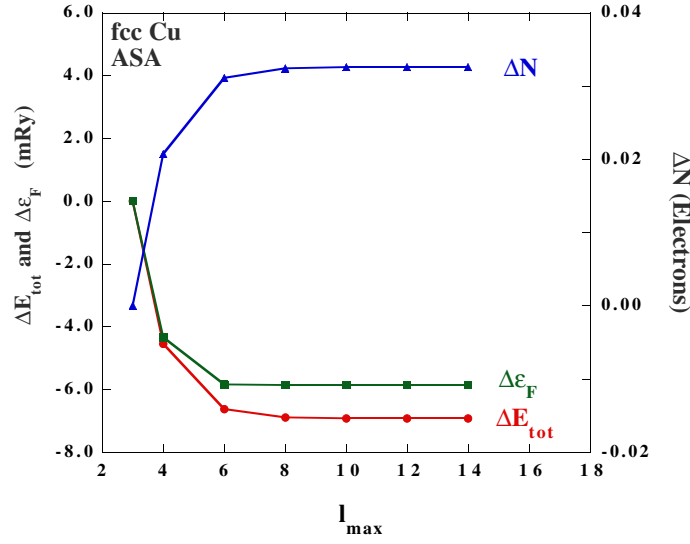


Figure 4. Convergence properties of ΔE_{tot} , $\Delta \epsilon_F$, and ΔN as functions of the maximum angular momentum cut-off l_{max} . Calculations for $l_{max} = 3$ are used as a reference. The results are for fcc Cu, $a = 6.76$ Bohr, the ASA, and $\Gamma = 87$.

same behaviour beyond $l_{max} = 4$. In the MT approximation, the density of states is calculated by integrating the Green's function (equation (1)) over the Voronoi polyhedron rather than the atomic sphere. In a cubic system, this results in off-diagonal contributions to the density of states, coupling, for example, the $l = 0$ to $l = 4$ and $l = 6$ components. Contrary to expectation for diagonal elements of the density of states which we have argued above should be small and positive for large values of l , these off-diagonal contributions can have either sign. It is these off-diagonal elements that give rise to the different behaviour in the MT case.

So far we have studied the convergence properties for a fixed lattice parameter. Of more significance is how the convergence of physical quantities such as the ground-state energy and equilibrium lattice parameter are affected. In figure 5, we show results for total energy as a function of lattice spacing for $3 \leq l_{max} \leq 12$. The results are for fcc copper in the MT approximation. While there are large differences between the curves for $l_{max} = 3, 4$, and 8 , the curves for $l_{max} = 8$ and 12 are essentially identical.

Equilibrium lattice parameters a_0 , ground-state total energies E_0 , and bulk moduli B_0 corresponding to the data shown in figure 5 are presented in table 2.

Table 2. Equilibrium lattice constant a_0 , bulk modulus B_0 , and total energy E_0 for fcc and bcc copper at several values of l_{max} . Calculations use the MT approximation and $\Gamma = 87$ (89) for fcc (bcc) structure.

l_{max}	fcc			bcc		
	a_0 (Bohr)	B_0 (Mbar)	E_0 (Ryd)	a_0 (Bohr)	B_0 (Mbar)	E_0 (Ryd)
3	6.764	1.672	-3275.76616	5.383	1.635	-3275.76505
4	6.727	1.716	-3275.77162	5.345	1.689	-3275.76916
8	6.749	1.664	-3275.76430	5.360	1.646	-3275.76288
12	6.747	1.604	-3275.76439	5.361	1.645	-3275.76283

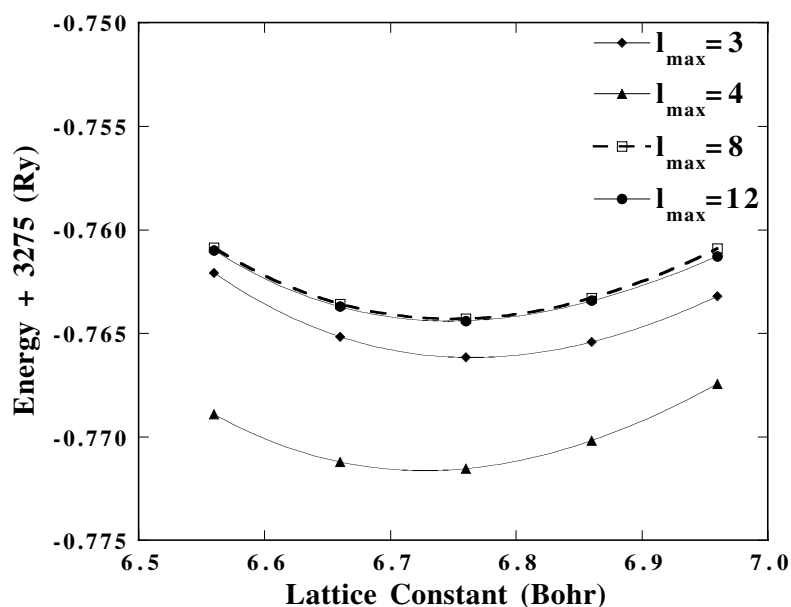


Figure 5. Total energies calculated at four values of l_{max} as functions of the lattice parameter for fcc copper (MT approximation).

The equilibrium quantities for fcc and bcc lattices are converged at $l_{max} = 8$. For the fcc structure the errors in energy and lattice constant are of the order of 0.09 mRyd and 0.002 Bohr while the bulk modulus is converged to within 0.06 Mbar. The corresponding errors are somewhat smaller for the bcc structure. Note that the $l_{max} = 4$ results exhibit the largest error with respect to the fully converged $l_{max} = 12$ values.

4. Conclusions

The above studies show that KKR Green's function calculations do not converge as rapidly, with the angular momentum, as has generally been assumed, even for the case of spherical approximations to the crystal potential. A high level of convergence (<0.04 mRyd) appears to be attained at $l_{max} \geq 12$. However, accurate total energies, lattice constants, and bulk moduli can be obtained at $l_{max} = 8$. For this l_{max} , the errors in energy, lattice constant, and bulk modulus are of the order of 0.1 mRyd, 0.002 Bohr, and 0.1 Mbar per atom in the fcc structure and are slightly smaller for the bcc structure. Obviously, even this degree of accuracy may not be necessary in some cases. The difference between the total energy calculated at $l_{max} = 8$ and the total energy calculated at the conventional $l_{max} = 3$ is about 2 mRyd for both fcc and bcc structures at the lattice parameters tested. Total energies for $l_{max} = 4$ show the largest error (about 7 mRyd) compared to those obtained at $l_{max} = 8$.

Since the calculations performed here utilize spherical approximations to the cell potential, the question may arise of whether the above results will remain valid for general shape potentials. In a recent study, Zeller *et al* calculate total energies as functions of lattice constant for metallic copper and aluminium at $l_{max} = 4, 6,$ and 8 using the full-potential TB KKR method [7]. The energy curves for aluminium, shown in their figure 1, exhibit behaviour similar to those in figure 5, i.e., the total energy at $l_{max} = 4$ shows underbinding compared with that obtained at $l_{max} = 8$ by ~ 5 – 6 mRyd. This is in good agreement with the MT results

presented here. Thus it appears that the large l_{max} required to obtain highly converged energies, etc, does not result from the non-spherical terms in the potential, t -matrices, etc, but is intrinsic to MST even for the case of spherical approximations.

Before closing, it is worthwhile to comment on how the findings in this paper affect the standing of KKR-based calculations in general. Clearly, this depends on the details of how they are performed. If the single-centre expansion is used throughout, then the considerations detailed here apply. If the Fermi energy is determined from the Lloyd formula and the single-centre expansion is used for the charge density, then the reliability of the results depends on how the resulting charge discrepancy is treated. For MT calculations this is easily hidden by assigning it to the interstitial region. For ASA and full-potential calculations, no such option exists.

Recently, a new version of the LMTO method has been proposed [14, 15] that continues to use a spherical approximation to the single-site potential while giving a good approximation to full-potential calculations. In this method, which closely resembles the TB KKR method, the single scatterer is extended even beyond the ASA radius [16]. Given this, it is clear that close attention should be paid to the l -convergence properties of this new method.

Acknowledgments

The work performed at Oak Ridge National Laboratory was supported by the Office of Basic Energy Sciences, Division of Materials Science and Engineering, and Office of Advanced Scientific Computing Research, Mathematics, Information and Computational Sciences Division, US Department of Energy. Oak Ridge National Laboratory is operated by UT-Battelle, LLC, for the US Department of Energy under contract DE-AC05-00OR22725.

References

- [1] Korringa J 1947 *Physica* **13** 392
- [2] Kohn W and Rostoker N 1954 *Phys. Rev.* **94** 1111
- [3] Butler W H, Dederichs P H, Gonis A and Weaver R L 1992 *Applications of Multiple Scattering Theory to Materials Science (Mater. Res. Soc. Symp. Proc. 253)* (Pittsburgh, PA: Materials Research Society)
- [4] Nicholson D M C, Stocks G M, Wang Y, Shelton W A, Szotek Z and Temmerman W M 1994 *Phys. Rev. B* **50** 14686
- [5] Wang Y, Stocks G M, Shelton W A and Nicholson D M C 1995 *Phys. Rev. Lett.* **75** 2867
- [6] Abrikosov I A, Niklasson A M N, Simak S I, Johansson B, Ruban A V and Skriver H L 1996 *Phys. Rev. Lett.* **76** 4203
- [7] Zeller R, Asato M, Hoshino T, Zabloudil J, Weinberger P and Dederichs P H 1998 *Phil. Mag.* **B 78** 417
- [8] Asato M, Settels A, Hoshino T, Asada T, Blugel S, Zeller R and Dederichs P H 1999 *Phys. Rev.* **60** 5202
- [9] Butler W H 1990 *Phys. Rev. B* **41** 2684
- [10] Faulkner J S and Stocks G M 1980 *Phys. Rev. B* **21** 3222
- [11] Györfy B L and Stott M J 1973 *Band Structure Spectroscopy of Metals and Alloys* ed D J Fabian and L M Watson (New York: Academic) p 385
- [12] Moghadam N Y, Stocks G M, Ujfalussy B, Shelton W A, Gonis A and Faulkner J S 1999 *J. Phys.: Condens. Matter* **11** 5505
- [13] Lloyd P 1967 *Proc. Phys. Soc.* **90** 207
- [14] Andersen O K, Saha-Dasgupta T, Tank R W, Arcangeli C, Jepsen O and Krier G 1999 *Preprint cond-mat/9907064*
Andersen O K, Saha-Dasgupta T, Tank R W, Arcangeli C, Jepsen O and Krier G 2001 *Springer Lecture Notes in Physics* ed H Dreyse (Berlin: Springer) at press
- [15] Andersen O K and Saha-Dasgupta T 2000 *Phys. Rev. B* **62** R16 219
(Andersen O K and Saha-Dasgupta T 2001 *Preprint cond-mat/0010454*)
- [16] Vitos L, Skriver H L, Johansson B and Kollar J 2000 *Comput. Mater. Sci.* **18** 24